p-Tolyl[α-^{13}C]diazomethane. Decomposition of [*carbaldehyde*-^{13}C]-*p*-tolualdehyde tosylhydrazone sodium salt gave *p*-tolyl[α-^{13}C]diazomethane (0.1 g, 0.3 mmol) as described in the formation of *o*-tolyl[α-^{13}C]diazomethane.

Thermolysis of p-Tolyl[α-^{13}C]diazomethane. Thermolysis of *p*-tolyl[α-^{13}C]diazomethane as described for *o*-tolyl[α-^{13}C]diazomethane gave styrene (98%), *p*-xylene (1%), and benzene (1%) in 79% overall yield by GLC and GC/MS analyses. The ^{13}C NMR ($CDCl_3$) spectrum of the final product is assigned[10] as follows: 128.31 (meta carbon of styrene) and 127.79 (para carbon of styrene). A repeat experiment gave similar results within experimental error.

Thermolysis of [2.2]Paracyclophane. Thermolysis of [2.2]paracyclophane (61 mg, 0.29 mmol) under the same conditions used for the thermolysis of [α-^{13}C]benzocyclobutene afforded 33 mg products. GLC and GC/MS analyses showed styrene (55%), *p*-xylene (31%), benzene (4%), benzocyclobutene (4%), and toluene (3%).

Thermolysis of [2.2]Metacyclophane. Thermolysis of [2.2]metacyclophane[32] (57 mg, 0.27 mmol) under the same conditions used for the thermolysis of [α-^{13}C]benzocyclobutene afforded 32 mg products. GLC and GC/MS analyses showed styrene (18%), *p*-xylene (35%), *m*-xylene (3%), benzocyclobutene (1%), benzene (7%), and toluene (22%).

Thermolysis of [2.2]Metaparacyclophane. Thermolysis of [2.2]metaparacyclophane[33] (28 mg, 0.13 mmol) under the same conditions used for the thermolysis of [α-^{13}C]benzocyclobutene gave 17 mg of products. GLC and GC/MS analyses showed styrene (10%), *p*-xylene (63%), *m*-xylene (1%), benzocyclobutene (1%), benzene (3%), and toluene (15%).

p-Ethyl[*carboxy*-^{13}C]benzoic Acid. The procedure described for the synthesis of [*carboxy*-^{13}C]-*o*-toluic acid gave *p*-ethyl[*carboxy*-^{13}C]benzoic acid (6.74 g, 44.6 mmol, 89%) from *p*-bromoethylbenzene (18.51 g, 100 mmol), magnesium turnings (6.15 g, 256 mmol), and 99% ^{13}C barium carbonate (9.87 g, 50.0 mmol): bp 111.5-113 °C; ^{1}H NMR ($CDCl_3$) δ 1.26 (t, 3 H, J_{H-H} = 7 Hz), 2.73 (q, 2 H, J_{H-H} = 7 Hz), 7.29 (d, 2 H, J_{H-H} = 8 Hz), 8.04 (dd, 2 H, J_{H-H} = 8, $J_{^{13}C-H}$ = 4 Hz), 12.30 (br s, 1 H); mass spectrum (70 eV), *m/e* (relative intensity) 152 (4), 151 (44, M^+), 136 (45), 135 (2), 107 (26), 106 (14), 105 (100), 91 (25), M^+ calcd 151.0715, obsd 151.0719; ^{13}C NMR ($CDCl_3$) δ 172.45 (^{13}COOH).

p-Ethyl[α-^{13}C]benzyl Alcohol. Reduction of *p*-ethyl[*carboxy*-^{13}C]-benzoic acid (1.34 g, 8.9 mmol) as described for the reduction of [*carboxy*-^{13}C]-*o*-toluic acid gave *p*-ethyl[α-^{13}C]benzyl alcohol (1.21 g, 8.8 mmol, 99%) as a colorless liquid: bp 144-146 °C/30 torr; ^{1}H NMR ($CDCl_3$) δ 1.23 (t, 3 H, J_{H-H} = 7 Hz), 1.82 (br s, 1 H), 2.66 (q, 2 H, J_{H-H} = 7 Hz), 4.65 (d, 2 H, $J_{^{13}C-H\alpha}$ = 144 Hz), 7.19-7.50 (m, 4 H); ^{13}C NMR ($CDCl_3$) δ 65.08 ($^{13}CH_2OH$).

p-Ethyl[α-^{13}C]benzyl Chloride. Reaction of *p*-ethyl[α-^{13}C]benzyl alcohol (1.21 g, 8.8 mmol) with concentrated hydrochloric acid as described in the formation of *o*-methyl[α-^{13}C]benzyl chloride gave *p*-ethyl[α-^{13}C]benzyl chloride (1.33 g, 8.5 mmol, 97%): bp 105-107 °C/30 torr; ^{1}H NMR ($CDCl_3$) δ 1.30 (t, 3 H, J_{H-H} = 7 Hz), 2.71 (q, 2 H, J_{H-H} = 7 Hz), 4.62 (d, 2 H, $J_{^{13}C-H\alpha}$ = 152 Hz), 7.10-7.50 (m, 4 H); ^{13}C NMR ($CDCl_3$) δ 46.23 ($^{13}CH_2Cl$).

p-Ethyl[α-^{13}C]toluene. Dropwise addition of *p*-ethyl[α-^{13}C]benzyl chloride (1.35 g, 8.7 mmol) in 87 mL of dimethyl sulfoxide to a well-stirred solution of sodium borohydride (1.64 g, 44 mmol) in 87 mL of dimethyl sulfoxide gave a clear solution. Stirring (6 h) at room temperature, dilution with distilled water (100 mL), extraction with ether, drying (Na_2SO_4), filtration, concentration under reduced pressure, and distillation gave *p*-ethyl[α-^{13}C]toluene (0.84 g, 6.9 mmol, 80%) as a colorless liquid: bp 160-163 °C; ^{1}H NMR ($CDCl_3$) δ 1.33 (t, 3 H, J_{H-H} = 7 Hz), 2.74 (q, 2 H, J_{H-H} = 7 Hz), 2.45 (d, 3 H, $J_{^{13}C-H\alpha}$ = 126 Hz), 7.10-7.40 (m, 4 H); mass spectrum (70 eV), *m/e* (relative intensity) 122 (3), 121 (26, M^+), 106 (100), 105 (23), 92 (14), 91 (2), M^+ calcd 121.0973, obsd 121.0980; ^{13}C NMR ($CDCl_3$) δ 20.93 ($Ar^{13}CH_3$).

Thermolysis of p-Ethyl[α-^{13}C]toluene. Neat *p*-ethyl[α-^{13}C]toluene (121 mg, 1.00 mmol), thermolyzed under exactly the same conditions as the pyrolysis of [α-^{13}C]benzocyclobutene, gave 93 mg of products. GLC and GC/MS showed styrene (5.7%), benzene (0.8%), toluene (6.7%), ethylbenzene (5.1%), *p*-xylene (16.2%), starting material (34.5%), *p*-methylstyrene (26.5%), indene (0.3%), phenylacetylene (0.5%), benzocyclobutene (0.3%), and 1-methylene-4,4-dimethylcyclohexadiene (0.3%). The ^{13}C NMR ($CDCl_3$) spectrum of the final products is assigned[10] as follows: δ 136.54 (α carbon of styrene), 128.31 (meta carbon of styrene), 127.79 (para carbon of styrene), 125.82 (ortho carbon of styrene), 113.34 (β carbon of styrene), 128.30 (benzene), 21.36 (methyl carbon of toluene), 15.52 (β carbon of ethylbenzene), 28.84 (α carbon of ethylbenzene), 21.03 (methyl carbon of *p*-xylene), 20.93 (aromatic methyl carbon of *p*-ethyltoluene), 28.46 ($^{13}CH_2CH_3$ of *p*-ethyltoluene), 15.73 ($CH_2{}^{13}CH_3$ of *p*-ethyltoluene), 21.15 (methyl carbon of *p*-methylstyrene), 136.75 (α carbon of *p*-methylstyrene), and 112.70 (β carbon of *p*-methylstyrene). A repeat experiment gave similar results within experimental error.

Acknowledgment. Mobile Chemical Co. and the National Science Foundation (Grant CHE 81 11196) supported this research. We are indebted to Professor W. S. Trahanovsky for a preprint of his manuscript.

Registry No. Benzocyclobutene, 694-87-1.

(33) Cram, D. J.; Hefelfinger, D. T. *J. Am. Chem. Soc.* **1971**, *93*, 4754-4763.

(34) McMahon, R. J. Ph.D. Dissertation, University of California, Los Angeles, Los Angeles, CA, 1985.

A Theoretical Study of Proton Transfer in Lithium Carbonyl and Lithium Enolate Complexes

Michael L. McKee

Contribution from the Department of Chemistry, Auburn University, Auburn, Alabama 36849.
Received May 19, 1986

Abstract: MNDO and ab initio (3-21+G) calculations have been used to study the mechanism of deprotonation of acetaldehyde by lithium amide to form the lithium enolate amine complex. The transition structure, which is characterized by a nearly colinear C-H-N arrangement involving the transferring proton, is predicted to be very reactant-like, suggesting that the cis to trans ratio can be predicted from differences in the conformational energy in the carbonyl compounds. The reverse reaction, the intramolecular protonation of the enolate to reform acetaldehyde, is predicted to be endothermic by 30.2 kcal/mol (3-21+G). However, the reaction of the enol with the lithium-amine complex is predicted to be exothermic by 16.3 kcal/mol. The observed *intramolecular* proton transfer in acid solution can be rationalized by solvent (H_2O) deprotonation of oxygen concurrent with protonation of nitrogen as the concerted proton transfer proceeds.

The stereoselectivity of enolate formation from carbonyl compounds using lithium compounds has received much attention.[1-17] The ratio of geometric isomers can be altered by changing the countercation,[5] the solvent,[15] and the size of the substituents on

0002-7863/87/1509-0559$01.50/0

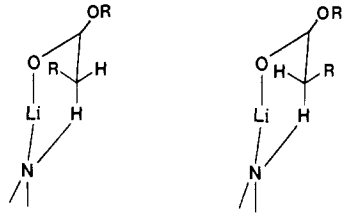

Figure 1. (a, left; b, right) Model transition structures for enolate formation proposed by Ireland.

the carbonyl carbon and on the carbon to which the departing hydrogen is attached.[12] Ireland[7] has proposed a model (Figure 1) which rationalizes the predominant formation of the trans isomer[8] in THF under conditions of kinetic control. Intramolecular steric repulsion between R and the carbonyl group favors the transition structure model in Figure 1a over that in Figure 1b. In a more strongly coordinating solvent such as HMPA–THF the lithium is less strongly coordinated to the carbonyl oxygen, and a bulky group on the carbonyl carbon will favor the staggered orientation in Figure 1b over that in Figure 1a (thermodynamic control[7b,15]). The model has been criticized[9] because the base does not attack along the C–H axis, which is expected to be more favorable.

Using a molecular mechanics model, Moreland and Dauben[10] have been able to predict successfully the stereoselective outcome of lithium enolate formation. They assume a linear relationship between the energy difference in conformations of the carbonyl compound and the activation barrier. On the basis of a closer relationship between the derived activation barrier difference and the calculated conformational energy difference for model carbonyl compounds than for corresponding model enols, the authors predicted that the transition structure will be reactant-like.

Also, asymmetric induction has been accomplished[11b,12-17] through the use of compounds where intramolecular complexation between lithium and the carbonyl oxygen is possible, creating a chiral environment. Reaction products may then have a definite stereochemistry due to specific geometric constraints in the transition structure caused by lithium complexation. Since proton abstraction from ketones to form enolates of known stereochemistry is a basic operation in organic synthesis, there is clearly a need to understand the role of the lithium amide deprotonation reagent, which is modeled in the present study as lithium amide rather than the frequently encountered lithium diisopropylamide (LDA).

While the stereochemical outcome of the reaction is known to be solvent dependent, the mechanism predicted in the gas phase may apply to the solution phase. Recent theoretical studies of lithium compounds[18,19] have shown that solvation energies, while sensitive to steric effects, are structure independent. Thus, dicoordinated lithium compounds may be expected to have similar solvation energies provided the steric requirements of the ligands are similar. The degree of aggregation in a particular solvent will be determined by a compromise of increasing stabilization through self-association into dimers, trimers, etc., and a loss of solvation energy as the volume of access to lithium is decreased.[19]

The present study was undertaken to study the energetics and geometric requirements of the deprotonation of acetaldehyde by lithium amide. In a recent study of the reaction of acetaldehyde with a different lithium compound, lithium hydride, it was found[20] that the hydride adds to the carbonyl carbon, forming an ethoxide which is complexed to lithium. A barrier of 8.4 kcal/mol was calculated with respect to the reactant complex which was 29.0 kcal/mol more stable than monomers (3-21G*). The difference in the two pathways may be due to the fact that the conjugate acid of amide (an amine) continues to bind strongly to lithium while the conjugate acid of hydride (H_2) does not, thereby favoring the deprotonation pathway by amide but not by hydride.

Method

The combination of semiempirical (MNDO)[21] and ab initio methods[22] has proven to be effective in studying reactions involving lithium complexation.[23-26] Optimizations are very rapid at the MNDO level and allow the calculation of a potential energy surface which reproduces all qualitative features of the more accurate ab initio surface. The use of MNDO geometries followed by a single-point calculation at the 3-21+G level (3-21+G//MNDO) yields a potential energy surface within several kcal/mol of the fully optimized surface (3-21+G//3-21+G) at a small fraction of the computer cost.[25,26] In contrast, the MNDO potential energy surface may differ from the 3-21+G//3-21+G surface by almost 20 kcal/mol (vide infra). The results obtained below justify the use of MNDO geometries (not energies), provided allowances are made for certain known shortcomings of MNDO. One such shortcoming is the known tendency to predict lithium interactions with carbon too stable by

(1) Wakefield, B. J. In *Comprehensive Organometallic Chemistry*; Wilkinson, G., Ed.; Pergamon: New York, 1982; Vol. 7, pp 1–110.
(2) Wakefield, B. J. *The Chemistry of Organolithium Compounds*; Pergamon: Oxford, 1974.
(3) Baigrie, L. M.; Seiklay, H. R.; Tidwell, T. T. *J. Am. Chem. Soc.* **1985**, *107*, 5391–5396.
(4) (a) Beak, P.; Kempf, D. J.; Wilson, K. D. *J. Am. Chem. Soc.* **1985**, *107*, 4745–4756. (b) Beak, P.; Hunter, J. E.; Jun, Y. M. *J. Am. Chem. Soc.* **1983**, *105*, 6350–6351.
(5) (a) House, H. O.; Czuba, L. J.; Gall, M.; Olmstead, H. D. *J. Org. Chem.* **1969**, *34*, 2324. (b) House, H. O.; Trost, B. M. *J. Org. Chem.* **1965**, *30*, 1341.
(6) (a) D'Angelo, J. *Tetrahedron* **1976**, *32*, 2979–2990. (b) Jackman, L. M.; Lange, B. C. *Tetrahedron* **1977**, *33*, 2737–2769.
(7) (a) Ireland, R. E.; Mueller, R. H.; Willard, A. K. *J. Am. Chem. Soc.* **1976**, *98*, 2868–2877. (b) Corey, E. J.; Gross, A. W. *Tetrahedron Lett.* **1984**, *25*, 495–498.
(8) The terms cis and trans will be used to refer to the disposition of the non-hydrogen α-substituent and the carbonyl carbon.
(9) Narula, A. S. *Tetrahedron Lett.* **1981**, *22*, 4119–4122.
(10) Moreland, D. W.; Dauben, W. G. *J. Am. Chem. Soc.* **1985**, *107*, 2264–2273.
(11) (a) Meyers, A. I. *Aldrichimica Acta* **1985**, *18*, 59–68 and references cited therein. (b) Meyers, A. I. *Pure Appl. Chem.* **1979**, *51*, 1255–1268.
(12) (a) Heathcock, C. H.; Buse, C. T.; Kleschick, W. A.; Pirrung, M. C.; Sohn, J. E.; Lampe, J. *J. Org. Chem.* **1980**, *45*, 1066. (b) Evans, D. A.; Nelson, J. V.; Vogel, E.; Taber, T. R. *J. Am. Chem. Soc.* **1981**, *103*, 3099.
(13) Shirai, R.; Tanaka, M.; Koga, K. *J. Am. Chem. Soc.* **1986**, *108*, 543–545.
(14) Stork, G.; Shiner, C. S.; Cheng, C.-W.; Polt, R. L. *J. Am. Chem. Soc.* **1986**, *108*, 304–305.
(15) Fataftah, Z. A.; Kopka, I. E.; Rathke, M. W. *J. Am. Chem. Soc.* **1980**, *102*, 3959–3960.
(16) Houk, K. N.; Paddon-Row, M. N.; Rondan, N. G.; Wu, Y.-D.; Brown, F. K.; Spellmeyer, D. C.; Metz, J. T.; Li, Y.; Loncharich, J. *Science (Washington, D.C.)* **1986**, *231*, 1108–1117.
(17) Morrison, J. D.; Mosher, H. S. *Asymmetric Organic Reactions*; American Chemical Society: Washington, DC, 1976. *Asymmetric Synthesis*; Morrison, J. D., Ed.; Academic: New York, 1984; Vol. 2 and 3. Morrison, J. D.; Mosher, H. S. *Science (Washington, D.C.)* **1983**, *221*, 1013.
(18) Kaufmann, E.; Tidor, B.; Schleyer, P. v. R. *J. Comp. Chem.* **1986**, *7*, 334–344.
(19) Kaneti, J.; Schleyer, P. v. R.; Clark, T.; Kos, A. J.; Spitznagel, G. W.; Andrade, J. G.; Moffat, J. B. *J. Am. Chem. Soc.* **1986**, *108*, 1481–1492.
(20) Bachrach, S. M.; Streitwieser, A. *J. Am. Chem. Soc.* **1986**, *108*, 3946–3951.
(21) (a) Dewar, M. J. S.; Thiel, W. *J. Am. Chem. Soc.* **1977**, *99*, 4899–4907, 4907–4917. (b) Lithium parametrization: Thiel, W.; Clark, T., unpublished results.
(22) References to basis sets used are collected here. The program package GAUSSIAN 82 was used throughout: Binkley, J. S.; Frisch, M.; Raghavachari, K.; Fluder, E.; Seeger, R.; Pople, J. A., Carnegie-Mellon University. 3-21G basis: Binkley, J. S.; Pople, J. A.; Hehre, W. J. *J. Am. Chem. Soc.* **1980**, *102*, 939. 3-21+G basis: Clark, T.; Chandrasekhar, J.; Spitznagel, G.; Schleyer, P. v. R. *J. Comput. Chem.* **1983**, *4*, 294.
(23) (a) Schleyer, P. v. R. *Pure Appl. Chem.* **1984**, *56*, 151–162. (b) Schleyer, P. v. R. *Pure Appl. Chem.* **1983**, *55*, 355–362. (c) Sapse, A.-M.; Kaufmann, E.; Schleyer, P. v. R.; Gleiter, R. *Inorg. Chem.* **1984**, *23*, 1569–1574. (d) Wilhelm, D.; Clark, T.; Schleyer, P. v. R. *J. Chem. Soc. Chem. Commun.* **1983**, 211–214. (e) Jemmis, E. D.; Chandrasekhar, J.; Würthwein, E.-U.; Schleyer, P. v. R. *J. Am. Chem. Soc.* **1982**, *104*, 4275–4276. (f) Schleyer, P. v. R.; Kos, A. J.; Kaufmann, E. *J. Am. Chem. Soc.* **1983**, *105*, 7617–7623. (g) Boche, G.; Decher, G.; Etzrodt, H.; Dietrich, H.; Mahdi, W.; Kos, A. J.; Schleyer, P. v. R. *J. Chem. Soc., Chem. Commun.* **1984**, 1493–1494. (h) Kos, A. J.; Clark, T.; Schleyer, P. v. R. *Angew. Chem., Int. Ed. Engl.* **1984**, *23*, 620–621. (i) Hagopian, R. A.; Therien, M. J.; Murdoch, J. R. *J. Am. Chem. Soc.* **1984**, *106*, 5753–5754.
(24) Boche, G.; Wagner, H.-U. *J. Chem. Soc., Chem. Commun.* **1984**, 1591–1592.
(25) McKee, M. L. *J. Am. Chem. Soc.* **1985**, *107*, 859–864.
(26) McKee, M. L. *J. Am. Chem. Soc.* **1985**, *107*, 7284–7290.

Table I. Heats of Formation (kcal/mol) and Absolute Energies (−hartree) Calculated for Various Species

molecule	notation	symm	MNDO(NEV)[a]	3-21+G//MNDO	3-21+G//3-21+G	Δ[b]
NH_3		C_{3v}	−6.3 (0)	55.887 42	55.892 49	3.18
NH_4^+		T_d	165.0 (0)	56.236 56	56.236 56	0.00
$LiNH_2$		C_{2v}	8.0 (0)	62.716 50	62.717 18	0.43
$LiNH_3^+$		C_{3v}	115.9 (0)	63.149 04	63.152 26	2.02
H_2O		C_{2v}	−60.9 (0)	75.617 71		
LiOH		$C_{\infty v}$	−30.2 (0)	82.489 67		
$CH_3C(H)O(X)Y$						
$CH_3C(H)O$	1	C_s	−42.4 (0)	152.077 76	152.079 86	1.32
X = H^+	2	C_s	139.4 (0)	152.377 20	152.381 39	2.63
X = Li^+	3	C_s	75.5 (0)	159.344 97	159.351 92	4.36
X = $LiNH_2$	4	C_s	−51.1 (0)	214.828 91	214.836 95	5.05
X = $LiNH_3^+$	5	C_s	39.1 (0)	215.269 04	215.304 96	5.60
X = $LiNH_2$, Y = H^+	6	C_s	148.0 (0)	215.104 46		
X = LiOH	7	C_s	−113.2 (0)	234.604 88		
$H_2C{=}C(H)O(X)Y^-$						
$H_2C{=}C(H)O^-$	8	C_s	−36.0 (0)	151.485 03	151.487 66	1.65
X = H^+	9	C_s	−34.9 (0)	152.065 30	152.068 97	2.30
X = Li^+	10	C_s	−39.5[c] (0)	158.945 28	158.950 27	3.13
X = $LiNH_3^+$	11	C_s	−66.3[d] (0)	214.877 16	214.885 11	4.99
X = H^+, Y = H^+	12	C_s	160.2 (0)	152.365 34	152.363 81	4.69
X = H^+, Y = Li^+	13	C_s	87.1 (0)	159.304 86	159.323 17	11.49
X = H^+, Y = $LiNH_3^+$	14	C_s	49.5 (0)	215.257 75	215.279 04	13.36
X = $LiOH_2^+$	15	C_s	−118.0 (0)	234.602 26		
SS_1[e]	A	C_s	−24.5 (2)	214.794 91	214.804 08	5.76
TS_2	B	C_1	−28.0 (1)	214.808 82	214.821 98	8.26
TS_3	C	C_1	148.9 (1)	215.106 68		
TS_4(O-prot)	D	C_1		215.179 16		
TS_5(N-prot)	E	C_1		215.128 03		
TS_6	F	C_1	−77.9 (1)	234.566 28		
TS_7	G	C_1	56.3 (1)	151.933 26	151.939 16	3.70

[a] Number of negative eigenvalues of MNDO force constant matrix. [b] Energy stabilization (kcal/mol) at the 3-21+G level obtained by using the optimized 3-21+G geometry rather than the MNDO geometry. [c] The global MNDO minimum is a C_1 structure, 8.6 kcal/mol more stable and characterized by lithium bridging the oxygen and methylene positions. [d] The global MNDO minimum is a C_1 structure, 3.4 kcal/mol more stable and characterized by lithium bridging the oxygen and methylene positions. [e] Supersaddle point, characterized by two negative eigenvalues of the MNDO force constant matrix.

Table II. Energies of Association (kcal/mol) Calculated at Various Levels

monomers → complex	MNDO	3-21+G// MNDO	3-21+G// 3-21+G	Δ[a]	monomers → complex	MNDO	3-21+G// MNDO	3-21+G// 3-21+G	Δ[a]
1 + $LiNH_2$ → **4**	16.7	21.75	25.05	3.30	**2** + $LiNH_2$ → **6**	−0.6	6.75		
8 + $LiNH_3^+$ → **11**	146.2	152.59	153.85	1.25	**1** + $LiNH_3^+$ → **5**	34.4	43.46	45.72	2.26
10 + NH_3 → **11**	20.5	27.91	26.58	1.33	**3** + NH_3 → **5**	30.1	39.95	38.01	−1.94
13 + NH_3 → **14**	31.3	41.10	39.78	−1.31	**10** + H_2O → **15**	12.8	24.65		
2 + $LiNH_3^+$ → **14**	31.5	27.25	36.29	9.04	**1** + LiOH → **7**	40.6	23.51		

[a] The calculated difference in association energy obtained when 3-21+G geometries are used rather than MNDO geometries at the 3-21+G level.

Table III. Activation Barriers (kcal/mol) Calculated for Proton Transfer between Complexes at Various Levels

reactant complex → product complex	forward barrier			reverse barrier		
	MNDO	3-21+G// MNDO	3-21+G// 3-21+G	MNDO	3-21+G// MNDO	3-21+G// 3-21+G
4 $\xrightarrow{B}$ **11**[a]	23.1 (3.5)	12.61 (8.73)	9.40 (11.24)	38.3	42.90	39.63
14 $\xrightarrow{C}$ **6**	98.5	94.83		0.9	−1.39	
14 $\xrightarrow{D}$ **5**		49.31			73.36	
14 $\xrightarrow{E}$ **5**		81.42			105.46	
15 $\xrightarrow{F}$ **7**	40.1	22.58		35.3	24.23	
1 $\xrightarrow{G}$ **9**	98.7	90.70	88.32	91.2	82.88	81.48

[a] The first value is the barrier using the C_1 transition structure B while the second value is the energy difference between the C_1 transition structure and the C_s stationary structure A.

approximately 30 kcal/mol,[23b] leading in some instances to unrealistic geometries. The global minimum at the MNDO level may then involve an attractive lithium–carbon interaction that is absent in the ab initio optimized geometry.

It is known that BSSE (basis set superposition error[27,28]) increases the stability of lithium bridging compounds since the atomic orbitals of lithium in a bridging position can simultaneously supplement the atomic basis set of several atoms.[19,29] The addition of a set of diffuse *s* and *p* functions to very non-hydrogen atom reduces this effect significantly and is recommended for systems with significant charge separation.[30-32]

Basis set superposition error does not seem to be significant in MNDO

(27) Boys, S. F.; Bernardi, F. *Mol. Phys.* **1970**, *19*, 553–566.
(28) Carsky, P.; Urban, M. *Ab Initio Calculations*; Lecture Notes in Chemistry; Springer-Verlag: Heidelberg, 1980; Vol. 16.
(29) Würthwein, E.-U.; Sen, K. D.; Pople, J. A.; Schleyer, P. v. R. *Inorg. Chem.* **1983**, *22*, 496–503.
(30) Clark, T.; Chandrasekhar, J.; Spitznagel, G.; Schleyer, P. v. R. *J. Comput. Chem.* **1983**, *4*, 294–301.
(31) Waterman, K. C.; Streitwieser, A. *J. Am. Chem. Soc.* **1984**, *106*, 3138–3140.
(32) Bachrach, S. M.; Streitwieser, A. *J. Am. Chem. Soc.* **1984**, *106*, 2283–2287.

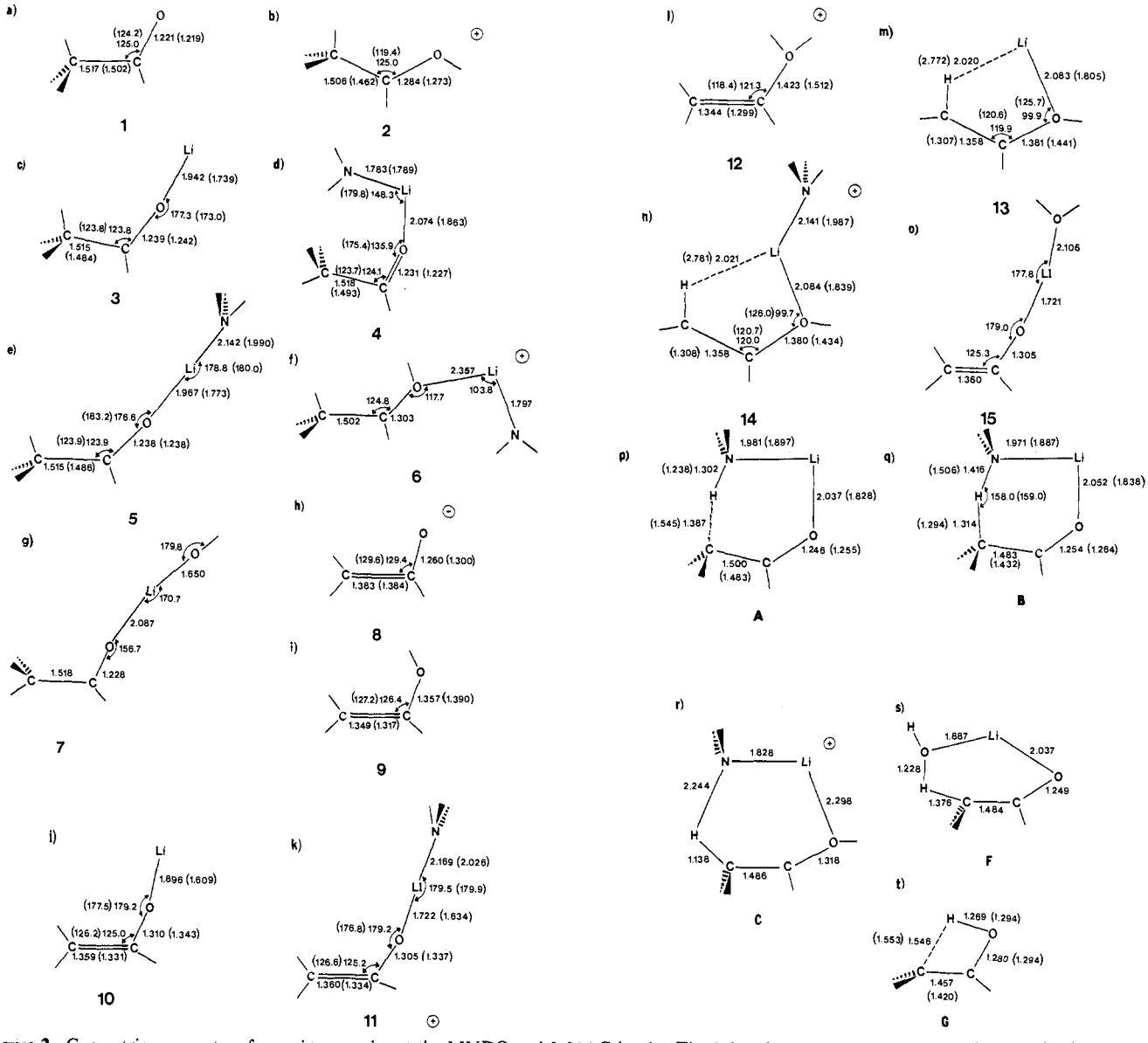

Figure 2. Geometric parameters for various species at the MNDO and 3-21+G levels. The 3-21+G parameters are in parentheses. The designated notation is consistent with that used in Tables I–III and in the text.

since dimerization and complexation energies agree well with experiment and with higher level ab initio calculations.[25] Total energies and heats of formation are tabulated in Table I for monomers and complexes, while association energies are given in Table II and reaction barriers are given in Table III. Selected geometric parameters at the MNDO and 3-21+G levels are given in Figure 2. A notation system has been adopted (numbers for stable geometries and letters for transition structures) and is used consistently in the tables and text.

Deprotonation of Acetaldehyde by Lithium Amide

Reactions involving lithium can be viewed artificially in three phases: (1) the reactants assemble in a reactant complex, (2) the reactant complex is transformed into the product complex, and (3) the product complex dissociates into monomers. In the present study the reactant complex will be between a lithium monomer and the oxygen of a second monomer. Depending on the coordinating ability of the solvent,[33] the actual reactant complex may be composed of a lithium aggregate (dimer, tetramer, hexamer, etc.) and the oxygen-containing monomer, which may then pass over a barrier to form a product complex.[26] Calculations of the methylation of formaldehyde by methyllithium and methyllithium dimer indicate that the barrier heights are very similar.[34] The possibility that in a highly coordinating solvent such as HMPA–THF the reaction may involve a bimolecular pathway with no reactant or product complex formation occurring is unlikely since it is known that lithium enolates can be trapped in the presence of HMPA.[7b] Also, there is indirect evidence[10] that the deprotonation of a ketone in HMPA–THF solution is predicted to go via a cyclic transition structure (which includes a lithium–oxygen interaction).

The association energy of acetaldehyde and lithium amide is calculated to be 25.0 kcal/mol at the 3-21+G//3-21+G level. In comparison the association between formaldehyde and methyllithium is calculated to be 27.7 kcal/mol (3-21G//3-21G)[35] and between formaldehyde and lithium methylamide is calculated to be 23.0 kcal/mol (3-21+G//3-21+G).[26] The potential energy surface is rather flat for distortions of the NLiO and LiOC angles. The MNDO-optimized NLiO and LiOC angles of the reactant complex **4** are 146.3° and 135.9° while at the 3-21+G level the optimum angles are 179.8° and 175.4°, respectively (Figure 2). Yet the energy at the 3-21+G level decreases only 5.0 kcal/mol

(33) For a recent MNDO study of solvation effects in lithium complexes, see: Kaneti, J.; Schleyer, P. v. R.; Clark, T.; Kos, A. J.; Spitznagel, G. W.; Andrade, J. G.; Moffat, J. B.; *J. Am. Chem. Soc.* **1986**, *108*, 1481–1492.

(34) Kaufmann, E.; Schleyer, P. v. R.; Houk, K. N.; Wu, Y.-D. *J. Am. Chem. Soc.* **1985**, *107*, 5560–5562.

(35) Del Bene, J. E.; Frisch, M. J.; Raghavachari, K.; Pople, J. A.; Schleyer, P. v. R. *J. Phys. Chem.* **1983**, *87*, 73–78.

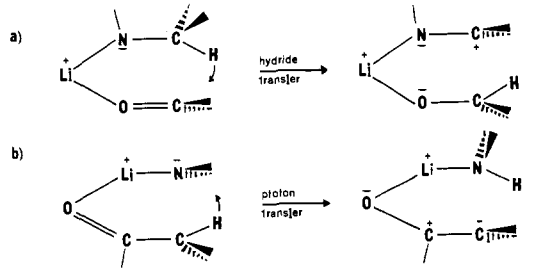

Figure 3. (a) Symmetry-allowed hydride transfer to formaldehyde from lithium methylamide. (b) Symmetry-allowed proton transfer from acetaldehyde to lithium amide.

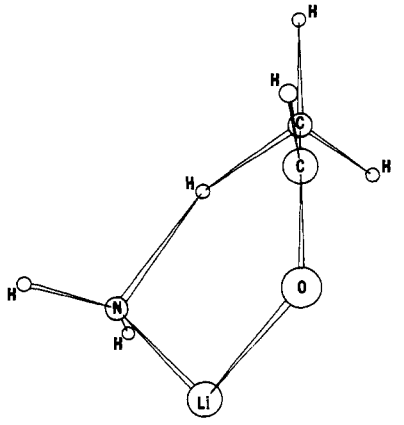

Figure 4. Plot of the transition structure B for proton abstraction from acetaldehyde by lithium amide. The symmetry is C_1, and the methyl group is approximately staggered with respect to oxygen.

when the 3-21+G geometry is used rather than the MNDO geometry.

The proton abstraction can take place through a six-membered cyclic transition structure A which is symmetry allowed as shown in Figure 3 along with a related hydride transfer from lithium methylamide to formaldehyde.[26] As the proton is transferred while maintaining a plane of symmetry, the zwitterion $C^-H_2C^+HOLi$ is formed. Rotation of the methylene would complete the formation of the enolate ion. Similar to the hydride transfer, the planar stationary structure is characterized by two imaginary modes (1275*i* and 464*i* cm^{-1}, 3-21+G). The true transition structure B has C_1 symmetry and is 11.2 kcal/mol lower than the C_s stationary structure. The stabilization gained from the $C_s \rightarrow C_1$ distortion is due to partial π-bond formation. The transition structure is reactant-like, since the C–C bond length in the reactant complex decreases only 0.061 Å in going to the transition structure at the 3-21+G//3-21+G level (0.035 Å, MNDO) while the C–O bond lengthens only 0.037 Å (0.023 Å, MNDO). A plot of the C_1 transition structure (Figure 4) reveals a staggered methyl group with respect to oxygen which is known to be the rotational transition structure in acetaldehyde (0.8 kcal/mol barrier at the 3-21+G//3-21+G level). Thus, the reaction does not take place from the lowest energy conformation of acetaldehyde since the developing π-overlap is better when the departing hydrogen leaves perpendicular to the forming double bond. The early transition structure explains why linear correlations are found between the differences in conformational energies of the carbonyl compound calculated by using molecular mechanics and the ratio of cis and trans isomers[8] of the product enolate.

Bulky substituents on the α-carbon would be more stable in the trans orientation to oxygen, leading to a preference for the trans isomer, while a large substituent on the carbonyl carbon would stabilize a transition structure leading to the cis isomer (Figure 4).[36] To determine the energy difference with a substituent on the methyl group, standard values were choosen for a CH_3 group (C–C 1.59 Å, C–H 1.08 Å, and C–C–H 109.5°) and two single-point calculations were performed with the methyl group substituted for one of the two nontransferring hydrogens on the α-carbon. The energy of the constrained transition structure with the methyl group trans to the carbonyl carbon was 1.0 kcal/mol lower in energy than the structure with the hydrogen in the trans position. This difference would lead to approximately a 90:10 ratio in favor of the trans isomer[8] at −70 °C.

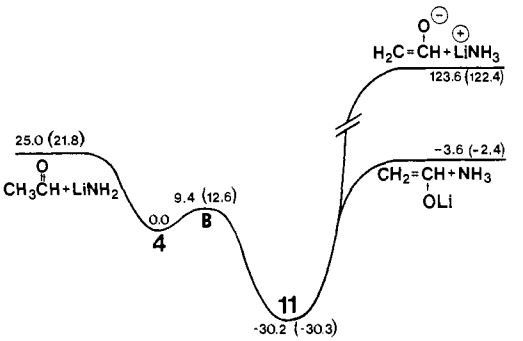

Figure 5. MERP (minimum energy reaction profile) at the 3-21+G//3-21+G level (3-21+G//MNDO) for proton abstraction from acetaldehyde by lithium amide to form an enolate.

The barrier for proton transfer is only 9.4 kcal/mol from the reactant complex **4** at the 3-21+G//3-21+G level (12.6 kcal/mol, 3-21+G//MNDO; 23.1 kcal/mol, MNDO). A low barrier is in agreement with the observed ease of reaction even at low temperature. Using the MNDO geometries for single-point calculations (3-21+G) increases the barrier slightly, while using the MNDO energies leads to a substantial overestimation of the barrier height.

It is interesting to note that Ireland's model[7] survives although the transition structure is not in a chair conformation. Since the electrostatic lithium–oxygen interaction is not very directional,[37] the lithium amide can swing around to allow proton abstraction while simultaneously maximizing the incipient C=C double bond formation (Figure 4). The resulting N–H–C bond angle (159.0°, 3-21+G; 158.7°, MNDO) is more in accordance with the linear orientation expected by Narula.[9]

For the product complex **11** there is significant disagreement between MNDO and ab initio methods as to the minimum energy structure. The lowest energy MNDO structure contains a lithium bridging the oxygen and methylene positions (see below). The

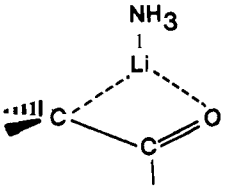

methylene is rotated, leaving a large negative charge on carbon while shifting the π-bond from C=C to C=O. Such a structure is reminiscent of several of the 1,3-dilithioacetone structures studied by Schleyer,[23h] which were not, however, the global minimum at the 3-21G level. An additional minimum energy structure at the MNDO level and 3.4 kcal/mol higher in energy is much closer to the 3-21+G//3-21+G optimized structure 11. In this structure the COLiN linkage is nearly linear, with lithium bound more tightly to the oxygen of the enolate than to the nitrogen of ammonia.

Two routes to monomers are possible. One is decomposition

(36) Schleyer, P. v. R.; Clark, T.; Kos, A. J.; Spitznagel, G. W.; Rohde, C.; Arad, D.; Houk, K. N.; Rondan, N. G. *J. Am. Chem. Soc.* **1984**, *106*, 6467–6475 and references cited therein.

(37) (a) See above discussion of the MNDO and 3-21+G geometries of the reactant complex **4**. (b) In a study of the reduction of formaldehyde by lithium borohydride, it was found that the energy of the reactant complex, $H_2C{=}O{-}Li{-}BH_4$, increased only slightly when the COLi and OLiB angles deviated widely from linearity. Bonaccorsi, R.; Palla, P. *THEOCHEM* **1982**, *87*, 181–196. (c) Amstutz, R.; Dunitz, J. D.; Laube, T.; Schweizer, W. B.; Seebach, D. *Chem. Ber.* **1986**, *119*, 434–443.

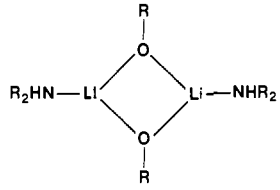

Figure 6. Structure of lithium ketone amide complex as determined by X-ray diffraction. The Li–N and Li–O distances are approximately 2.14 and 1.89 Å, respectively.

to $H_2C{=}C(H)OLi$ (**10**) plus NH_3, and the other is decomposition to $H_2C{=}C(H)O^-$ (**8**) plus $LiNH_3^+$. In the gas phase, the former is much lower in energy; however, in solution, the two pathways may be competitive. The complex **11** is 26.6 kcal/mol more stable than neutral monomers and 153.8 kcal/mol more stable than charged monomers at the 3-21+G//3-21+G level (27.9 and 152.6 kcal/mol, 3-21+G//MNDO; 20.5 and 146.2 kcal/mol, MNDO). A summary of energetics at the 3-21+G//3-21+G level is given in the form of a MERP (minimum energy reaction profile) in Figure 5.

The structure of the monomer, $H_2C{=}C(H)OLi$ (**10**), is by MNDO and ab initio methods in disagreement, in the same manner as the amine complex (product complex). The MNDO global minimum, a C_1 structure with a lithium bridge, is 1.8 kcal/mol more stable than a bridging structure of C_s symmetry and 8.6 kcal/mol more stable than the linearly coordinated enolate complex (**10**). At the MNDO level the C_s bridging structure is 6.8 kcal/mol more stable than the lithium enolate complex (**10**) while at the 3-21+G//3-21+G level the lithium enolate complex (**10**) is 33.8 kcal/mol more stable than the bridging structure.

Finally, enolates are known to form tetramers[38,39] or hexamers[40] in the solid state. A recent X-ray structure[41] of an enolate lithium amine dimer was characterized by a hydrogen bond between the hydrogen of the amine and the double bond of the enolate. The structure was interpreted[41] as a point on the reaction coordinate for concerted proton transfer, thus forming a ketone. In the simple product complex **11**, a NH---C=C hydrogen bond is not observed (Figure 2k). It is possible that the observed bridge becomes favorable only after dimer formation, which would considerably decrease the C–O–Li angle. The observed[41] Li–N and Li–O distances (Figure 6) are about 2.14 and 1.89 Å, respectively. In comparison the same values at the 3-21+G level for the simple complex **11** are 2.03 and 1.63 Å (2.17 and 1.72 Å, MNDO).

The reaction representing the intramolecular proton transfer from the amine to the enolate is just the reverse of the reaction discussed above (product complex **11** → reactant complex **4**). This reaction is thermodynamically unfavorable, being 30.2 kcal/mol endothermic (Figure 5) and having a barrier of 39.6 kcal/mol (3-21+G//3-21+G). It is known that in protic solvents, the transfer proceeds at least partially intramolecularly since only partial D^+ uptake is observed in the enolate using a D^+ source.[41,42] A possible mechanism for intramolecular transfer is shown in Figure 7. From the enol–lithium amine complex **14**, intramolecular transfer can take place to form the acetaldehyde–$LiNH_3^+$ complex **5**, which is predicted to be 16.3 kcal/mol exothermic at the 3-21+G//3-21+G level (24.0 kcal/mol, 3-21+G//MNDO; 10.4 kcal/mol, MNDO). During the course of reaction the O-protonated complex becomes N-protonated, thereby invoking

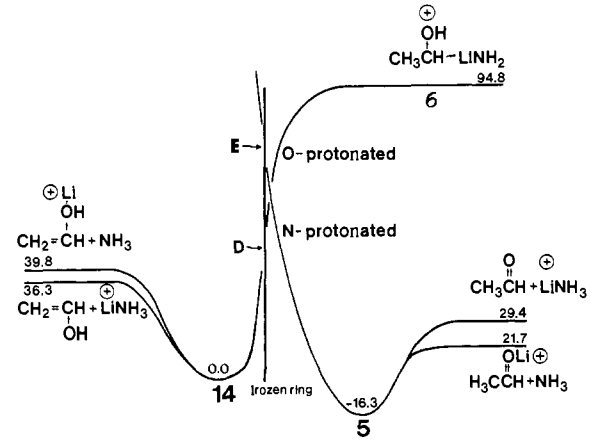

Figure 7. MERP at the 3-21+G//MNDO level for concerted proton transfer under acidic conditions. As the reaction proceeds along the "enolate" surface, the proton affinity of nitrogen will at some point exceed that of oxygen. Deprotonation of oxygen and protonation of nitrogen will cause a "jump" between surfaces and allow the formation of a thermodynamically more stable product complex. The two arrows correspond to calculations (D, E) at the 3-21+G//MNDO level obtained by adopting the ring portion from the unprotonated MNDO transition structure B and adding a proton to either the oxygen or the nitrogen.

active solvent participation (but not incorporation) during the concerted proton transfer.

Without solvent participation, intramolecular protonation is predicted to be very unfavorable, yielding $CH_3C(H)OH^+$ (**2**) plus $LiNH_2$. The barrier height is 94.8 kcal/mol, yielding a complex, **6** only 6.8 kcal/mol more stable than monomers at the 3-21+G//MNDO level (98.5 and −0.6 kcal/mol; MNDO). To estimate where the O-protonated and N-protonated "surfaces" cross, optimizations were carried out at the MNDO level, freezing the positions of the six atoms in the six-membered ring to their optimized position in the MNDO transition structure and adding a H^+ to either the oxygen or the nitrogen (Table III, D and E). The energy of the two calculations may bracket the lowest crossing (Figure 7). If the nitrogen is protonated too early along the intramolecular proton-transfer reaction coordinate, the nitrogen will be pentacoordinate. At a certain point, as the proton is transferred, the nitrogen will become increasing nucleophilic and enhance the probability of protonation on nitrogen. An alternative veiwpoint is that, as the reaction proceeds, the proton affinity of the nitrogen becomes greater than the proton affinity of oxygen. The two alternative paths for decomposition of the product complex are similar since in each case one neutral and one charged species is produced. The preferred decomposition path will be determined by the lithium cation affinity of $CH_3C(H){=}O$ compared to NH_3. Formation of $CH_3C(H)OLi^+$ (**3**) plus NH_3 is predicted to be 38.0 kcal/mol endothermic compared to 45.7 kcal/mol for formation of $CH_3C(H)O$ (**1**) plus $LiNH_3^+$ at the 3-21+G//3-21+G level (40.0 and 43.5 kcal/mol, 3-21+G//MNDO; 30.1 and 34.4 kcal/mol, MNDO). As shown in eq 1,

$$NH_3 + CH_3C(H){=}OLi^+ \rightarrow LiNH_3^+ + CH_3C(H){=}O \quad (1)$$

$$H_{rxn} = -7.7 \text{ kcal/mol}$$

the lithium cation affinity of NH_3 is calculated to be 7.7 kcal/mol greater than $CH_3C(H){=}O$. In a closely related reaction (eq 2),

$$NH_3 + H_2C{=}OLi^+ \rightarrow LiNH_3^+ + H_2C{=}O \quad (2)$$

the lithium cation affinity of NH_3 is 8.9 kcal/mol greater than $H_2C{=}O$ at the MP2/6-31G*//3-21G + ZPC/3-21G level and 3.1 kcal/mol experimentally.[35]

Proton transfer does not take place completely by intramolecular transfer from the amine to the enolate, as shown by partial deuterium incorporation.[41] Deuterium incorporation by the enolate in a D^+ source can take place either through direct deuteriation on carbon by a D^+ donor or through an exchange of the amine

(38) Seebach, D.; Amstutz, R.; Dunitz, J. D. *Helv. Chim. Acta* **1981**, *64*, 2622–2626.
(39) Amstutz, R.; Schweizer, W. B.; Seebach, D.; Dunitz, J. D. *Helv. Chim. Acta* **1981**, *64*, 2617–2621.
(40) Williard, P. G.; Carpenter, G. B. *J. Am. Chem. Soc.* **1986**, *108*, 462–468.
(41) Laube, T.; Dunitz, J. D.; Seebach, D. *Helv. Chim. Acta.* **1985**, *68*, 1373–1393.
(42) (a) Creger, P. L. *J. Am. Chem. Soc.* **1970**, *92*, 1396–1397. (b) Pfeffer, P. E.; Silbert, L. S.; Chirinko, J. M. *J. Org. Chem.* **1972**, *37*, 451. (c) Seebach, D.; Boes, M.; Naef, R.; Schweizer, W. B. *J. Am. Chem. Soc.* **1983**, *105*, 5390–5398. (d) Aebi, J. D.; Seebach, D. *Helv. Chim. Acta* **1985**, *68*, 1507–1518. (e) Strazewski, P.; Tamm, C. *Helv. Chim. Acta* **1986**, *69*, 1041–1051.

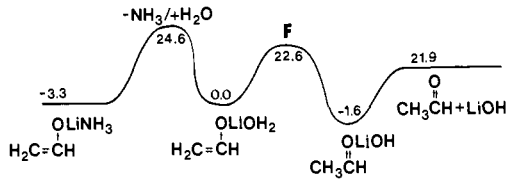

Figure 8. MERP at the 3-21+G//MNDO level for concerted proton transfer in the enolate–$LiOH_2$ complex to reform acetaldehyde. The barrier for dissociation of NH_3 in complex **11** is assumed to be the difference in energy of the complex and monomers. If NH_3 and D_2O exchange occurs, deuterium incorporation will be observed in acetaldehyde.

hydrogens with the solvent, which can transfer a deuterium to the enolate.

A calculation was made for the intramolecular proton transfer in the enolate–lithium water complex (reactant complex, **15**) to the acetaldehyde–lithium hydroxide complex (product complex, **7**). Ammonia is bound by 27.9 kcal/mol (3-21+G//MNDO) while water is bound by 24.6 kcal/mol. The difference in the calculated binding (3.3 kcal/mol) is similar to the calculated (6.5 kcal/mol)[35] and experimental (5.1 kcal/mol) difference between the binding energy of the lithium cation with ammonia and with water. The absolute binding is less since the positive charge of lithium is partially reduced through additional coordination to the $CH_2{=}C(H)O^-$ anion. The transition structure F for proton transfer from the coordinated water to carbon is of C_1 symmetry and is similar to B (Table I) except that the transferring proton is 1.228 Å from oxygen in F while it is 1.416 Å from nitrogen in B (MNDO geometries). The barrier is calculated to be 22.6 kcal/mol at the 3-21+G//MNDO level (40.1 kcal/mol, MNDO).[43] The product complex **15** is 1.6 kcal/mol more stable than the reactant complex **7** while the monomers, acetaldehyde and LiOH, are 23.5 kcal/mol less stable (Figure 8). While the concerted proton-transfer mechanism in the protonated lithium enolate–water complex was not investigated, it seems likely that if the amine is displaced, intramolecular proton transfer will readily occur. Therefore, the observation of incomplete deuterium incorporation requires that the amine–enolate exchange must be slow (or competitive) with respect to intramolecular proton transfer since otherwise total deuterium incorporation would result with a large excess of solvent (D_2O).

The concerted reaction, acetaldehyde ⇌ vinyl alcohol, was also studied[44] in order to emphasize that protonation by this pathway is unlikely. In the forward direction the barrier is 88.3 kcal/mol, and in the reverse direction it is 81.5 kcal/mol at the 3-21+G//3-21+G level (90.7 and 82.9 kcal/mol, 3-21+G//MNDO; 98.7 and 91.2 kcal/mol, MNDO). The C_1 transition structure G is characterized by a long C–H distance and a short O–H distance to the transferring hydrogen. Since the transition structure is strained and a hydrogen atom is transferred (rather than a proton), polarization and correlation may be important and would likely decrease the barrier height.

Acknowledgment. Computer time for this study was donated by the Auburn University Computer Center.

Registry No. Acetaldehyde, 75-07-0; lithium amide, 7782-89-0.

(43) A lower barrier may result with an additional water relaying the proton between the complexed water and the enolate; however, it is clear that with only one water molecule, incorporation of the proton from the solvent should result if water displaces the amine in the lithium enolate amine complex.

(44) For a CNDO/2 study of this reaction, see: Zakova, M.; Leska, J. *Collect. Czech. Chem. Commun.* **1983**, *48*, 433–438.